Cell Metabolism
Article

Mitochondrial Overload and Incomplete Fatty Acid Oxidation Contribute to Skeletal Muscle Insulin Resistance

Timothy R. Koves,[1,2] John R. Ussher,[4] Robert C. Noland,[1] Dorothy Slentz,[1] Merrie Mosedale,[1] Olga Ilkayeva,[1] James Bain,[1] Robert Stevens,[1] Jason R.B. Dyck,[4] Christopher B. Newgard,[1,2,3] Gary D. Lopaschuk,[4] and Deborah M. Muoio[1,2,3,*]

[1]Sarah W. Stedman Nutrition and Metabolism Center
[2]Department of Medicine
[3]Department of Pharmacology & Cancer Biology
Duke University, Durham, NC 27710, USA
[4]Cardiovascular Research Group, University of Alberta, Edmonton, AB T6G 2S2, Canada
*Correspondence: muoio@duke.edu
DOI 10.1016/j.cmet.2007.10.013

SUMMARY

Previous studies have suggested that insulin resistance develops secondary to diminished fat oxidation and resultant accumulation of cytosolic lipid molecules that impair insulin signaling. Contrary to this model, the present study used targeted metabolomics to find that obesity-related insulin resistance in skeletal muscle is characterized by excessive β-oxidation, impaired switching to carbohydrate substrate during the fasted-to-fed transition, and coincident depletion of organic acid intermediates of the tricarboxylic acid cycle. In cultured myotubes, lipid-induced insulin resistance was prevented by manipulations that restrict fatty acid uptake into mitochondria. These results were recapitulated in mice lacking malonyl-CoA decarboxylase (MCD), an enzyme that promotes mitochondrial β-oxidation by relieving malonyl-CoA-mediated inhibition of carnitine palmitoyltransferase 1. Thus, *mcd*$^{-/-}$ mice exhibit reduced rates of fat catabolism and resist diet-induced glucose intolerance despite high intramuscular levels of long-chain acyl-CoAs. These findings reveal a strong connection between skeletal muscle insulin resistance and lipid-induced mitochondrial stress.

INTRODUCTION

Insulin resistance, a state in which peripheral tissues are rendered unresponsive to the glucose-lowering, antilipolytic, and anabolic properties of the hormone, is a hallmark of obesity and type 2 diabetes. This condition typically develops in association with weight gain, prolonged physical inactivity, and/or systemic hyperlipidemia, thereby suggesting that the molecular underpinnings of insulin resistance might be driven by lipid surplus. Indeed, research over the past two decades has established a compelling connection between organ dysfunction and atypical storage of neutral lipids in tissues such as liver, heart, pancreas, and skeletal muscle (Muoio and Newgard, 2006).

The present investigation sought to advance our understanding of lipid-induced metabolic decline in skeletal muscle, a principal site of insulin-stimulated glucose clearance. Both in vitro and in vivo, exposure of skeletal muscle to an excessive lipid supply leads to intramuscular accumulation of fatty acid-derived metabolites and coincident lesions in insulin action (Hulver et al., 2003; Yu et al., 2002; Chavez et al., 2003). One prominent theory suggests that muscle insulin resistance arises from impaired mitochondrial uptake and oxidation of fatty acids (Morino et al., 2006; Ruderman et al., 1999). This model proposes that long-chain acyl-CoAs (LC-CoAs) derived from circulating lipids or intramuscular triacylglycerol (IMTG) are diverted away from carnitine palmitoyltransferase 1 (CPT1), the mitochondrial enzyme that catalyzes the first and essential step in β-oxidation of long-chain fatty acids, and are instead preferentially partitioned toward the synthesis of signaling intermediates such as diacylglycerol (DAG) and ceramide. Aberrant accumulation of these and other bioactive lipid molecules is thought to engage stress-activated serine kinases that interfere with insulin signal transduction (Holland et al., 2007; Yu et al., 2002).

Recent studies have challenged this theory by showing that genetic manipulations that increase tissue levels of these lipid molecules do not necessarily produce insulin resistance (An et al., 2004; Monetti et al., 2007). Moreover, emergent evidence from our laboratory suggests that obesity-associated glucose intolerance might arise from metabolic overload of muscle mitochondria (An et al., 2004; Koves et al., 2005a). This hypothesis was addressed herein using targeted metabolomics to assess lipid-induced metabolic dysfunction in both animal and cell culture models. Our results link the development of skeletal muscle insulin resistance to excessive rather than reduced β-oxidation and, moreover, suggest that fatty acids must penetrate muscle mitochondria to exert their insulin-desensitizing actions on this tissue. These findings suggest that pharmacologic strategies designed to boost β-oxidation be reconsidered.

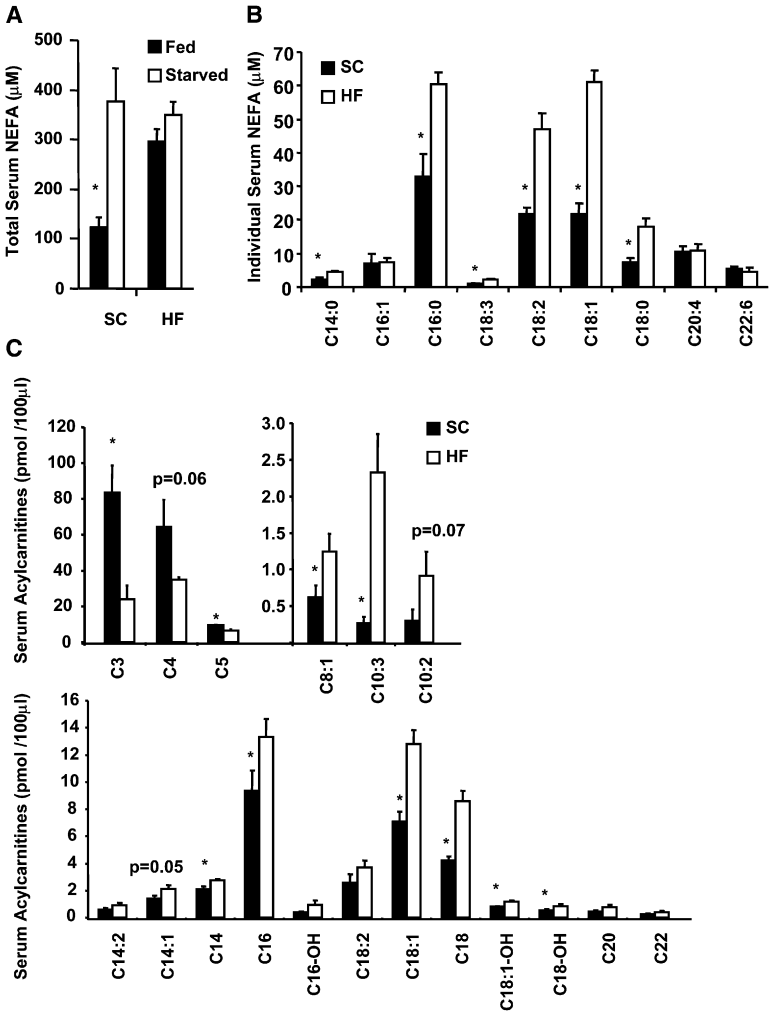

Figure 1. Chronic High-Fat Feeding Increases Postprandial Serum Nonesterified Fatty Acids and Acylcarnitines

Serum samples were harvested in the ad lib fed or 24 hr starved state from rats fed either standard chow (SC) or high-fat (HF) diet for 12 weeks. Data represent means ± SEM from 4–5 animals per group. *$p < 0.05$ relative to HF diet.

(A) Total nonesterified fatty acid (NEFA) levels.

(B) Individual serum NEFA species in the fed state measured by gas chromatography/mass spectrometry.

(C) Acylcarnitine species in the fed state measured by tandem mass spectrometry.

RESULTS

Obesity Is Characterized by Mitochondrial Lipid Overload

Animals fed a "western" high-fat (HF) diet for 12 weeks exhibited 23% increased body weight compared to standard chow (SC)-fed controls (633 ± 40 g and 515 ± 70 g in HF-fed versus SC-fed rats), which was accompanied by early-stage insulin resistance, mild hyperinsulinemia, hyperleptinemia, hypertriglyceridemia, and elevated glucocorticoid levels (An et al., 2004; Koves et al., 2005a). As expected, total serum nonesterified free fatty acids (NEFA) were elevated in response to an overnight fast and prolonged HF feeding; however, in the present study, the diet-induced increase was apparent only in the postprandial state (Figure 1A). Using gas chromatography/mass spectrometry (GC/MS), we then evaluated diet-induced changes in plasma levels of specific fatty acid species. Oleate (C18:1), palmitate (C16:0), linoleate (C18:2), and stearate (C18:0) were the most elevated fatty acids in HF-fed animals (Figure 1B).

Tandem MS/MS was then used to analyze 36 independent acylcarnitine species ranging in size from 2 to 22 carbons, representing byproducts of substrate catabolism. These acylcarnitine esters are formed from their respective acyl-CoA intermediates by a family of carnitine acyltransferases that reside in subcellular organelles (primarily mitochondria), where they catalyze the exchange of CoA for carnitine (Ramsay, 2000). Whereas acyl-CoAs cannot cross the mitochondrial membrane, the acylcarnitines do so efficiently. Subsequently, cytosolic acylcarnitines can be exported into the blood. The serum acylcarnitine profile therefore provides an integrated systemic snapshot of in vivo substrate flux through specific steps of β-oxidation and amino acid catabolism and is commonly used as a diagnostic tool for detecting inborn errors in metabolism (Van Hove et al., 1993).

Complete results of the serum acylcarnitine analysis are provided in Table S1 available online. Even-chain species ranging in length from C6 to C22 arise from incomplete β-oxidation of fatty acids. Odd-chain species such as C3 (propionylcarnitine) and C5 (isovalerylcarnitine) are produced during amino acid catabolism, whereas C4 (butyrylcarnitine) can be derived from both fatty acids and amino acids. Acetylcarnitine (C2) derives from acetyl-CoA, the universal degradation product of all metabolic substrates, and is thus the most abundant species in both tissues and blood. In response to overnight fasting, most lipid-derived acylcarnitines increased, whereas the amino acid intermediates decreased. Consistent with the fasting-induced rise in circulating NEFA, this profile implies a metabolic switch favoring higher rates of β-oxidation and diminished degradation of amino acids. Under fasting conditions, serum acylcarnitines were similar between the two diet groups. Conversely, serum samples collected in the fed state revealed higher levels of several fatty acid-derived species and reduced levels of C3, C4, and C5 in HF-fed animals compared to SC-fed animals (Figure 1C).

Skeletal muscle serves as a major reservoir of free carnitine and is thought to be a principal contributor to the serum acylcarnitine pool. We therefore evaluated acylcarnitine levels in the gastrocnemius, a representative muscle comprised of a mixture of type I, IIa, and IIb fibers. Consistent with the serum profile, we observed marked accumulation of fatty acylcarnitine species in muscles from HF-fed rats. Whereas SC-fed rats lowered most muscle fatty acylcarnitines during the transition from the fasted to the fed state, HF-fed animals exhibited little or no change (Figure 2A). Thus, during fasted conditions, the import of fatty acids into muscle mitochondria appears to exceed metabolic

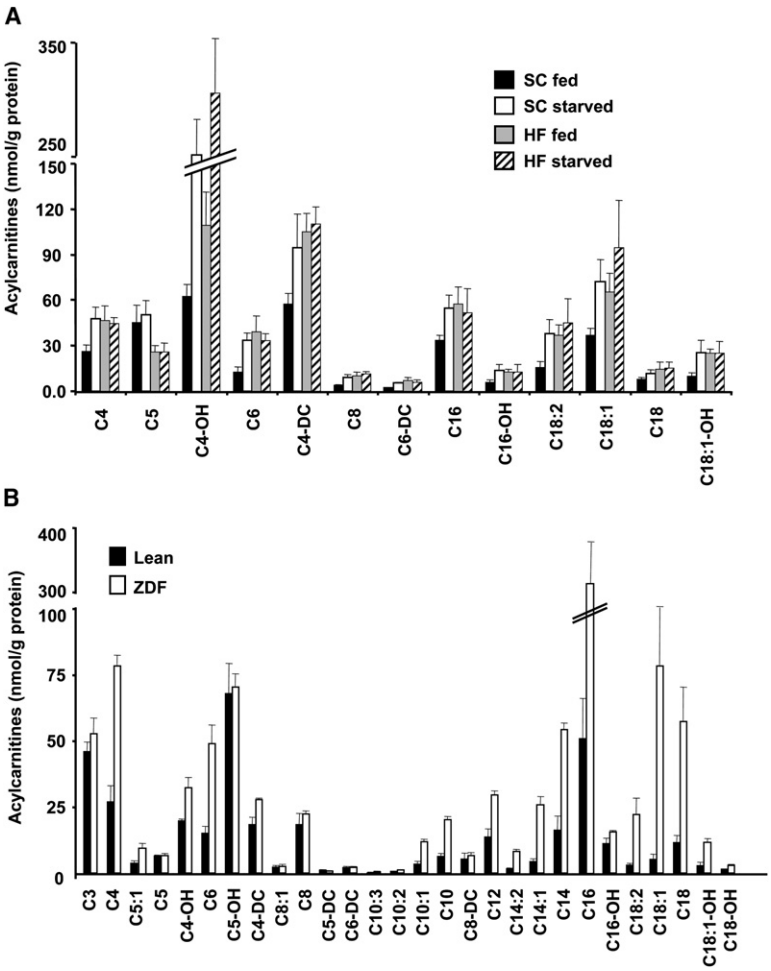

Figure 2. Skeletal Muscle Acylcarnitine Profiles Reveal Excessive β-Oxidation in Multiple Forms of Insulin Resistance

(A) Acylcarnitine levels in whole gastrocnemius muscles harvested in the ad lib fed or 24 hr starved state from rats fed either SC or HF diet for 12 weeks. Data represent means ± SEM from 4–5 animals per group.

(B) Acylcarnitine levels in whole gastrocnemius muscles harvested in the ad lib fed state from lean or obese Zucker diabetic fatty (ZDF) rats. Data represent means ± SEM from 3 animals per group.

Main effects of starvation ($p < 0.01$), diet ($p < 0.01$), and genotype ($p < 0.01$) were detected by two-way ANOVA or Student's t test, but symbols were excluded for simplicity.

demand. Feeding relieved the surplus, but only in the SC-fed group, suggesting that mitochondria from obese animals are unable to appropriately adjust fatty acid influx in response to nutritional status.

In contrast to skeletal muscle, liver acylcarnitines were not elevated in HF-fed animals compared to SC-fed animals (Figure S1A). Moreover, in SC-fed rats, long-chain acylcarnitine levels increased during the fed-to-fasted transition, consistent with increased CPT1 activity, whereas this response was impaired in the HF-fed group. Likewise, fasting-induced upregulation of CPT1α (the liver isoform) was abolished by HF feeding (Figure S1B). These data are consistent with the notion that liver fatty acid oxidation begins to fail within 12 weeks of overfeeding. We subsequently analyzed skeletal muscle and liver acylcarnitine levels in 15-month-old rats fed on the HF diet for 1 year, a model that mimics lifetime overnutrition in middle-aged humans. Upon prolonged HF diet exposure, fatty acid-derived acylcarnitines were uniformly and markedly decreased in liver but remained elevated in skeletal muscle (Figure S2). To determine whether this metabolite pattern might be common to more severe forms of insulin resistance, we next evaluated Zucker diabetic fatty (ZDF) rats, which develop obesity and diabetes secondary to hyperphagia and a mutation in the leptin receptor gene. Similar to in HF-fed animals, muscle acylcarnitine accumulation (Figure 2B) and mRNA levels of several β-oxidative genes (Figure S3) were elevated in obese ZDF animals as compared to their lean Zucker littermates. Together, these data support a model in which the development and progression of insulin resistance correspond with increased mitochondrial fatty acid catabolism in muscle but reduced fat oxidation in liver.

To gain further insight into diet-induced changes in muscle fuel metabolism, we used GC/MS to profile organic intermediates of glycolysis and the TCA cycle in skeletal muscle. The HF diet reduced levels of lactate, citrate, malate, and succinate (Figures 3A–3C). In general, concentrations of these organic acids were less responsive to nutritional status in HF-fed compared to SC-fed animals, although the interaction did not reach statistical significance. We also observed a similar trend of lower organic acid levels in gastrocnemius muscles from ZDF rats compared to control rats (Figure 3D). Analysis of these data sets by multivariate analysis of variance (MANOVA) revealed a main effect ($p < 0.05$) of diet and genotype when the TCA cycle intermediates were modeled as a group.

High-Fat Feeding Impairs Mitochondrial Control

Mitochondrial β-oxidative capacity was assessed using two distinct in vitro preparations. Crude measures of β-oxidation were initially performed in skeletal muscle homogenates prepared from red and white quadriceps femoris. As expected, oxidation rates of [^{14}C]oleate were several-fold higher in mitochondria-enriched red skeletal muscle (Figures 4A and 4B). The 12-week HF diet did not affect complete oxidation of oleate to CO_2. Radiolabel incorporation into acid-soluble metabolites (ASMs), which provides an index of incomplete fat catabolism (Koves et al., 2005a), was elevated after HF feeding as compared to SC feeding. This effect was more pronounced in white compared to red quadriceps.

Because the homogenate preparation does not account for differences in mitochondrial content or other nonmitochondrial enzymatic activities, we also evaluated rates of fatty acid catabolism in isolated mitochondria from the whole gastrocnemius. As described previously, mitochondria from HF-fed rats compared to SC-fed rats displayed similar rates of [^{14}C]oleate oxidation to CO_2 but accumulated more radiolabeled intermediates in the

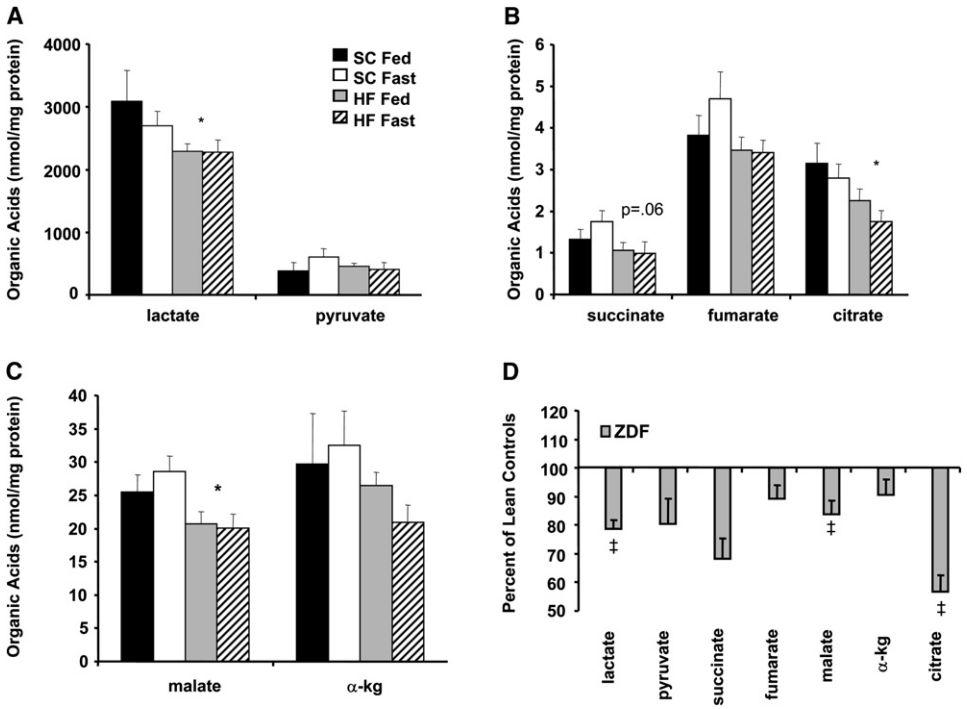

Figure 3. Skeletal Muscle Organic Acid Profiles Reveal Diminished Levels of TCA Cycle Intermediates in Multiple Forms of Insulin Resistance

(A–C) Organic acid levels in whole gastrocnemius muscles harvested in the ad lib fed or 24 hr starved state from rats fed either SC or HF diet for 12 weeks. Data represent means ± SEM from 4–5 animals per group. *$p < 0.05$ for main diet effect between individual species by two-way ANOVA.

(D) Organic acid levels in whole gastrocnemius muscles harvested in the ad lib fed state from lean Zucker and obese ZDF rats. Data are expressed as percent decrease in ZDF animals compared to lean control animals. Data represent means ± SEM from 9 animals per group. ‡$p < 0.05$ for genotype difference by Student's t test.

acid-soluble pool (Koves et al., 2005a). In the present experiments, we sought to simulate the transition between fasting and feeding by adding pyruvate to the incubation buffer as a competing glucose-derived carbon source (Figures 4C and 4D). In mitochondria from SC-fed animals, pyruvate caused an appropriate and robust inhibition of oleate oxidation, consistent with substrate switching as predicted by the "glucose-fatty acid cycle" (Randle et al., 1963). By contrast, this switch was nearly absent in mitochondria harvested from the HF-fed group.

Exposure to Fatty Acids Disrupts Mitochondrial Fuel Homeostasis in Cultured Myotubes

We next examined the consequences of lipid surplus in cultured myocytes. Rat L6 myotubes were exposed to 500 μM fatty acids, using an equimolar ratio of oleate and palmitate, the two most abundant fatty acids in serum of HF-fed rats (Figure 1). Carnitine was used as a nutritional tool to manipulate rates of β-oxidation. Carnitine is synthesized in the liver and sequestered in skeletal muscle at estimated concentrations of 2–3 mM, whereas carnitine stores in cultured myocytes are extremely low (Figure S4). It is noteworthy that many cell-based studies of insulin resistance have been performed in myocytes exposed to palmitate, but in the absence of carnitine and other unsaturated fatty acids (Chavez et al., 2003; Lee et al., 2006). Such conditions represent a severe departure from in vivo fuel metabolism and are likely to elicit cytotoxic responses (Rachek et al., 2007). The toxic effects of palmitate per se have been attributed to its low rate of incorporation into triacylglycerol (TAG), which in turn leads to abnormal accumulation of palmitoyl-CoA, DAG, and/or ceramide. As proof of this concept, Figure 5 shows changes in TAG content and glycerol release (a measure of TAG turnover) in L6 myotubes treated for 24 hr with palmitate compared to oleate with or without carnitine. TAG levels were below detection limits in control cells grown in standard medium (data not shown) and increased upon fatty acid exposure (Figure 5A). In the absence of supplemental carnitine, β-oxidation is severely restricted (Figure S1); thus, fatty acids are preferentially partitioned toward alternative biosynthetic fates. As predicted, TAG biosynthesis was much lower in cells exposed to palmitate as compared to oleate or the oleate-palmitate mix (Figures 5A and 5B). This low potential for TAG biosynthesis was accompanied by increased cell death as assessed by adenylate kinase leak into the medium (Figure 5C). Cell viability was partially or fully rescued when the addition of carnitine or oleate permitted enhanced utilization of palmitate for β-oxidation or TAG synthesis, respectively.

Exposure of L6 myotubes to high (500 μM) compared to low (100 μM) levels of fatty acids resulted in a disproportionate increase in the rate of incomplete ([^{14}C]oleate incorporation into ASMs) relative to complete ([^{14}C]oleate incorporation into CO_2) oxidation of fatty acids (Figure S4). Likewise, fatty acid surplus caused cultured myocytes to accumulate even-chain acylcarnitines of short, medium, and long chain length, whereas odd-chain species (C3 and C5) decreased (Figure 5D). Palmitoylcarnitine (C16) content was 3-fold greater than oleoylcarnitine

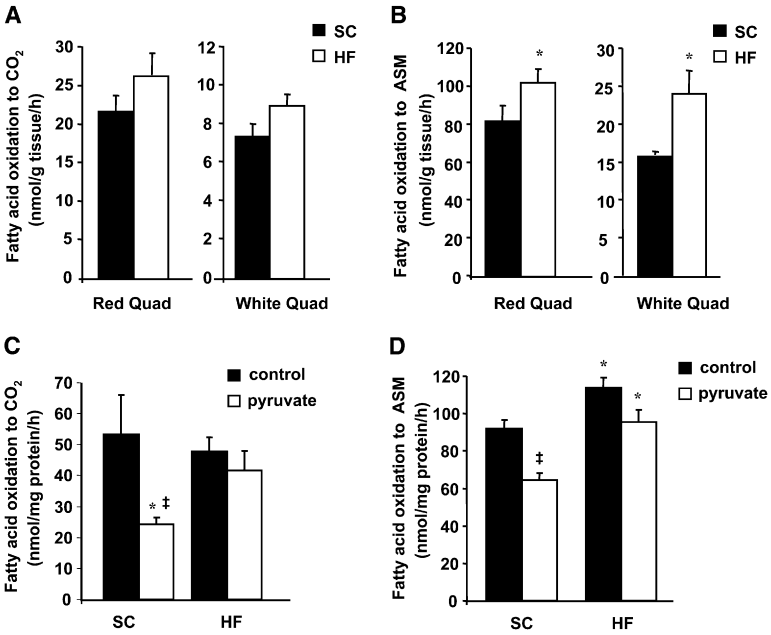

Figure 4. High-Fat Feeding Promotes Incomplete β-Oxidation and Metabolic Inflexibility in Skeletal Muscle

Muscles were harvested from rats fed either SC or HF diet for 12 weeks. Data represent means ± SEM from 4–5 animals per group. *$p < 0.05$ relative to SC diet; ‡$p < 0.05$ relative to no pyruvate condition.

(A) Complete oxidation of 200 μM [1-^{14}C]oleate to CO_2 in muscle homogenates prepared from deep (Red Quad) or superficial (White Quad) quadriceps.

(B) Incomplete oxidation of 200 μM [1-^{14}C]oleate to acid-soluble metabolites (ASM) in muscle homogenates prepared from deep (Red Quad) or superficial (White Quad) quadriceps.

(C) Complete oxidation of 200 μM [1-^{14}C]oleate to CO_2 in isolated mitochondria from whole gastrocnemius muscle, incubated with or without 2 mM pyruvate.

(D) Incomplete oxidation of 200 μM [1-^{14}C]oleate to ASM in isolated mitochondria from whole gastrocnemius muscle, incubated with or without 2 mM pyruvate.

(C18:1), suggesting that palmitate is a preferred substrate for β-oxidation. Taken together with Figure 5C, these data imply that acylcarnitine accumulation does not compromise cell viability. The lipid-induced changes in the acylcarnitine profile were fully prevented by coadministration of etomoxir, a potent inhibitor of CPT1 (Figure 5D). In sum, these results strongly suggest that incubating myocytes with a physiological blend of oleate, palmitate, and carnitine (as opposed to palmitate alone) better approximates the metabolic conditions observed in insulin-resistant animals.

Insulin Resistance in L6 Myocytes Requires β-Oxidation

To further examine the connection between incomplete fat oxidation and insulin resistance, L6 myotubes were pretreated for 24 hr with BSA or BSA complexed with 500 μM fatty acids in the presence or absence of 1 mM carnitine. Subsequently, [^{14}C]glucose metabolism was measured in cells provided with standard culture medium lacking exogenous fatty acids and carnitine. In BSA-treated control cells, insulin increased rates of glycogen synthesis but elicited only a minor elevation in glucose oxidation (Figures 5E and 5F). Both glucose oxidation and glycogen synthesis were inhibited 40%–50% by fatty acid exposure. Fatty acid-induced decrements in glycogen synthesis were similar under basal and insulin-stimulated conditions, such that the relative response to insulin (2.3-fold increase) was unchanged. Notably, the impairments in glucose metabolism were evident only when the fatty acid pretreatment was accompanied by supplemental carnitine.

Insulin signaling was evaluated following 24 hr preincubation with or without fatty acids and increasing carnitine concentrations. In the absence of fatty acids, acute insulin administration triggered robust phosphorylation of AKT (Ser473), a downstream molecule of the insulin signaling pathway that regulates translocation of the insulin-responsive glucose transporter, GLUT4. When carnitine was absent, exposure to fatty acids caused only a modest impairment in AKT activation despite elevated IMTG (Figure 5G). Conversely, resistance to insulin became progressively more severe when fatty acid treatment was combined with increasing doses of carnitine. Likewise, addition of etomoxir protected against the signaling impairment caused by the combination of fatty acid and carnitine (Figure 5H). These treatments did not affect total AKT abundance (Figure S4).

mcd$^{-/-}$ Mice Are Protected from Diet-Induced Glucose Intolerance

Malonyl-CoA decarboxylase (MCD) degrades the natural CPT1 inhibitor malonyl-CoA and thereby facilitates fatty acid import into mitochondria. Knockout mice lacking MCD activity therefore provide a genetic model of partial CPT1 inhibition. These animals were generated as described previously (Dyck et al., 2006) to examine the role of MCD in heart disease. Neither the *mcd*$^{+/-}$ heterozygous nor the *mcd*$^{-/-}$ mice displayed an overt phenotype (Dyck et al., 2006). As compared with wild-type animals, hearts from *mcd*$^{-/-}$ mice exhibited elevated malonyl-CoA levels, a marked preference for glucose utilization following ischemia, and improved cardiac function during recovery from ischemia/reperfusion.

Here, we used a metabolomics approach to evaluate the consequences of eliminating *mcd* in skeletal muscle. Ablation of *mcd* resulted in an 11-fold increase in muscle levels of malonylcarnitine (C3-DC) (Figure 6A), which is derived from malonyl-CoA. In the setting of an SC diet, levels of most other acylcarnitine intermediates in muscle were similar between genotypes (data not shown); however, distinct phenotypes emerged when animals were challenged with a HF diet to encourage fatty acid catabolism. Whereas muscles from wild-type mice had predictably high levels of several fatty acylcarnitines, loss of MCD activity prevented accumulation of most lipid-derived species (Figure 6B).

Muscle lactate levels were lower and pyruvate content trended higher in the *mcd*$^{-/-}$ mice compared to wild-type mice (Figure 6C). Interestingly, gastrocnemius muscles lacking *mcd*

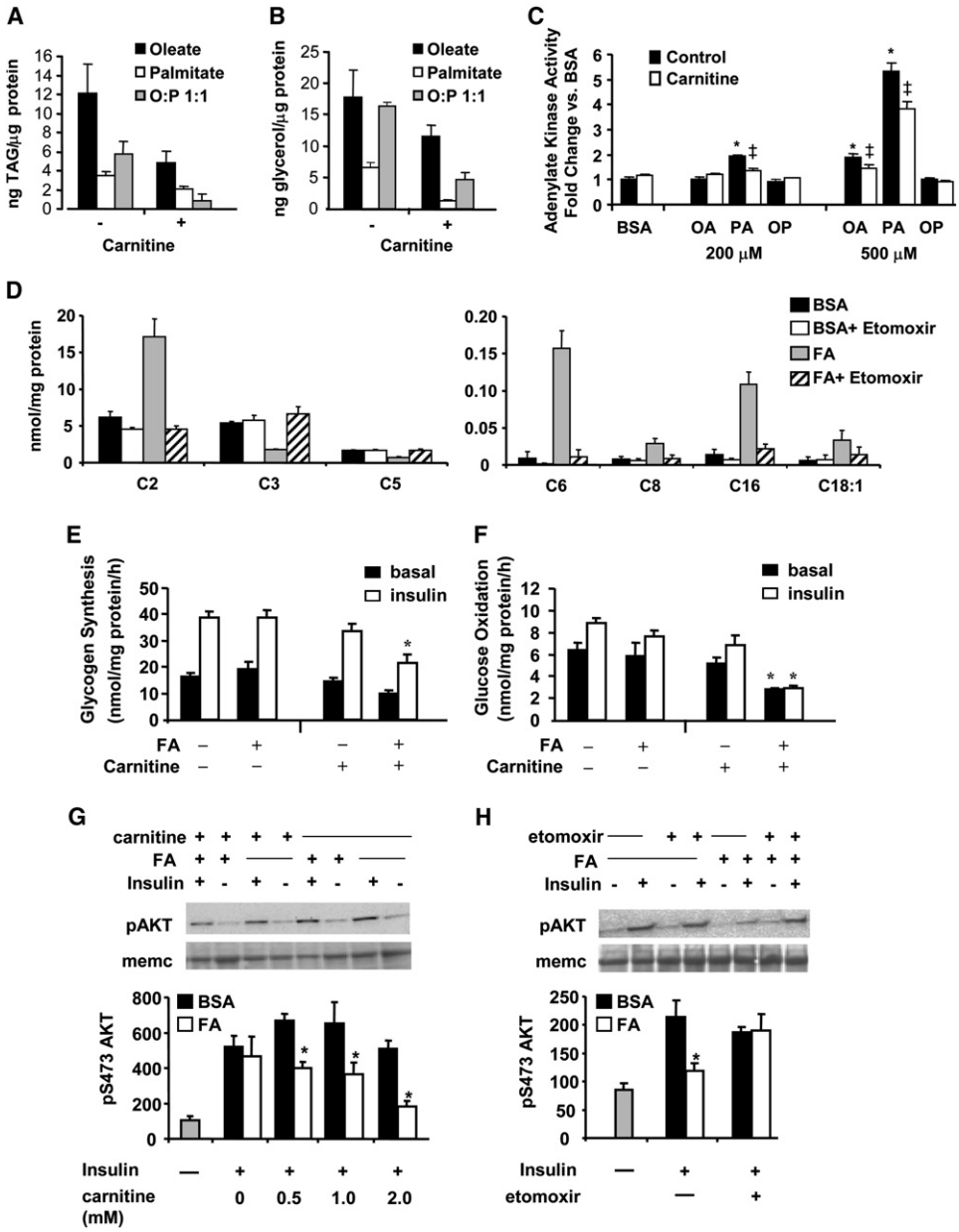

Figure 5. Fatty Acid Metabolism and Insulin Resistance in L6 Skeletal Myotubes

(A and B) Triacylglycerol (TAG) synthesis and turnover were assessed in L6 myotubes treated for 24 hr with 500 μM oleate, palmitate, or a 1:1 oleate:palmitate blend with or without 1 mM L-carnitine. Cellular triacylglycerol content (A) and glycerol release into medium (B) were quantified spectrophotometrically. Data represent means ± SD from two independent experiments performed in duplicate.

(C) Cytotoxicity was assayed by measuring adenylate kinase activity in the medium after 24 hr exposure to 0, 200, or 500 μM oleate (OA), palmitate (PA), or a 1:1 mix of oleate:palmitate (OP). Data are normalized to total adenylate kinase activity per well and represent means ± SD from two independent experiments performed in duplicate. *$p < 0.05$ relative to BSA control; ‡$p < 0.05$ relative to no carnitine condition.

(D) Acylcarnitine accumulation was measured in L6 myotubes treated with 1 mM L-carnitine and 0.5% BSA, alone or complexed with 500 μM oleate:palmitate (1:1) with or without 100 μM etomoxir. Data are presented as means ± SD from experiments performed in triplicate and are representative of at least two experiments with similar results.

(E and F) L6 myotubes were pretreated for 24 hr with 0.5% BSA alone or complexed with 500 μM 1:1 oleate:palmitate (FA) ± 2 mM L-carnitine, followed by a 2 hr incubation with [UL-^{14}C]glucose ± 100 nM insulin, to determine rates of glycogen synthesis (E) and glucose oxidation to CO_2 (F). Data are presented as means ± SD from experiments performed in triplicate and are representative of at least two experiments with similar results.

(G and H) L6 myotubes were pretreated for 24 hr with 0.5% BSA alone or complexed with 500 μM 1:1 oleate:palmitate and increasing concentrations of L-carnitine (G) or 2 mM carnitine ± 100 μM etomoxir (H), followed by 15 min stimulation ± 100 nM insulin and western blot analysis of phosphorylated AKT2. MemCode (memc) staining was used to normalize protein transfer. Data are means ± SD from experiments performed in triplicate and are representative of at least three other experiments with similar results. *$p < 0.05$ comparing fatty acid exposure to BSA under the respective conditions by Student's t test.

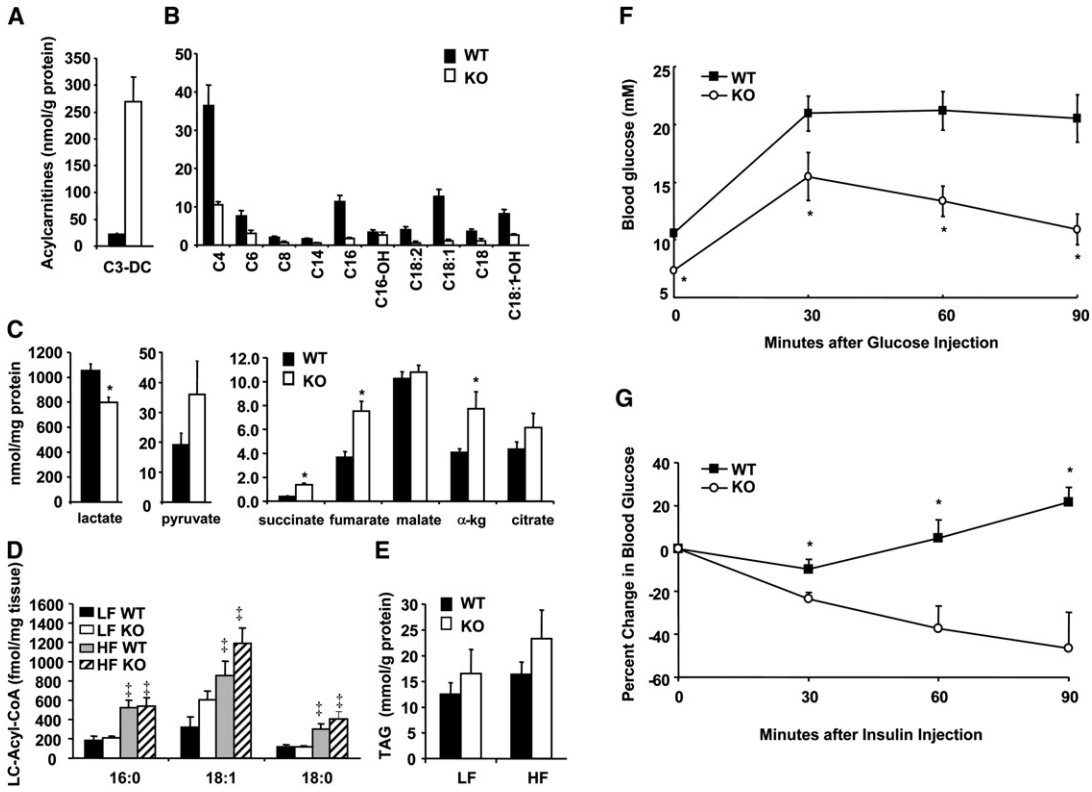

Figure 6. *mcd*$^{-/-}$ Mice Are Protected against Diet-Induced Glucose Intolerance

(A–C) Metabolic profiling was performed on gastrocnemius muscle lysates from wild-type (WT) and *mcd*$^{-/-}$ (KO) mice fed a HF diet for 12 weeks. Tissues were harvested in the postprandial state and analyzed for malonylcarnitine (A), fatty acylcarnitine species (B), and organic acids (C).

(D and E) Long-chain acyl-CoAs (LC-Acyl-CoA) (D) and TAG content (E) were measured in mice fed either low-fat (LF) or HF diet for 12 weeks.

(F and G) Whole-body glucose tolerance (F) and insulin sensitivity (G) tests were performed in mice fed a HF diet for 12 weeks.

*$p < 0.05$ versus WT; ‡$p < 0.05$ versus animals of same genotype on SC diet.

Data represent means ± SEM from 6 animals per group.

maintained higher levels of succinate, fumarate, and α-ketoglutarate in response to the HF diet, suggesting that excessive β-oxidation directly contributes to the low levels of these intermediates observed in insulin-resistant rodents. Diet-induced accumulation of LC-CoAs was evident in both wild-type and *mcd*$^{-/-}$ mice and tended to be amplified in the latter (Figure 6D). Intramuscular TAG content followed a similar trend (Figure 6E).

Insulin action was examined by glucose and insulin tolerance tests. Wild-type and *mcd*$^{-/-}$ mice responded similarly to these challenges when animals were fed the SC diet (data not shown); however, the HF regimen revealed striking genotype-specific responses. As expected, wild-type mice developed diet-induced insulin resistance, evidenced by elevated fasting blood glucose, impaired glucose tolerance, reduced insulin responsiveness, and rebound hyperglycemia following insulin administration (Figures 6F and 6G; Figure S5). In contrast, *mcd*$^{-/-}$ mice displayed remarkable protection against these metabolic perturbations. Thus, enhanced glucose utilization and insulin sensitivity in the knockout mice occurred in the face of high intramuscular lipid levels and diminished rates of β-oxidation.

To gain insight into changes in hepatic lipid metabolism, we profiled liver metabolites (Figure S6). As in skeletal muscle, levels of malonylcarnitine in liver were elevated in knockout mice compared to control mice. However, in general, the acylcarnitine, organic acid, and LC-CoA profiles revealed only modest metabolic differences between genotypes. Moreover, plasma ketone levels were similar between groups, indicating that hepatic β-oxidation was not severely compromised by the loss of *mcd*. We used indirect calorimetry to examine whole-body substrate utilization during the early phases of HF feeding. In wild-type mice, the HF diet caused a dramatic decrease in the respiratory exchange ratio (RER) (Figure 7A), indicative of increased fat oxidation. Similar to our experiments in rats, the HF regimen abolished the robust fluctuations in substrate selection apparent in control mice during transitions between light and dark cycles. These changes were evident within 2 weeks after initiating the diet and preceded insulin resistance as assessed by an insulin tolerance test (data not shown). Compared to their wild-type counterparts, *mcd*$^{-/-}$ mice fed the HF diet maintained a higher RER, reflecting elevated glucose oxidation, but only during the dark/active cycle, when systemic substrate use is more heavily influenced by skeletal muscle (Figure 7B). In the aggregate, ablation of *mcd* appears to confer partial inhibition of CPT1 that manifests selectively in skeletal muscle as compared to liver. Although these findings do not preclude the possibility that *mcd*$^{-/-}$ mice have enhanced hepatic insulin sensitivity, the weight of the evidence suggests that changes in skeletal

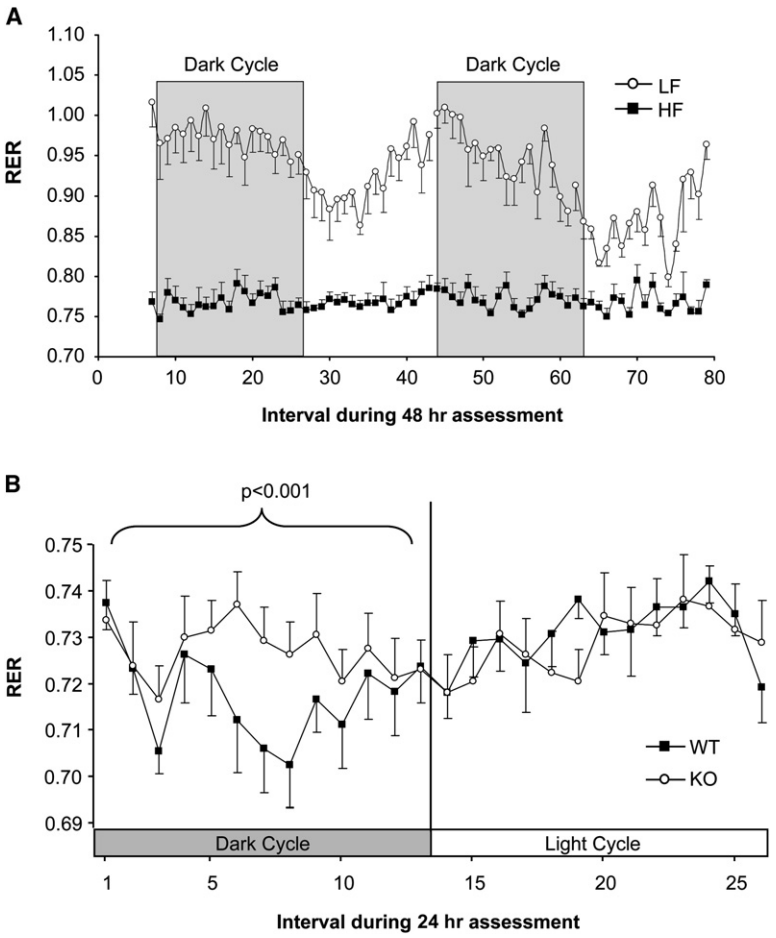

Figure 7. Whole-Body Substrate Oxidation in Wild-Type and *mcd*$^{-/-}$ Mice

Indirect calorimetry was performed using an eight-chamber Oxymax system (Columbus Instruments). Mice were acclimatized to the system prior to measurement. Respiratory exchange ratio (RER) was calculated as VCO_2/VO_2. Data represent means ± SEM from 6–11 animals per group.

(A) Wild-type mice were fed either a 10% fat (LF) or 60% fat (HF) diet for 2 weeks prior to whole-body metabolic assessments. Measurements were recorded every 40 min.

(B) *mcd*$^{-/-}$ (KO) and wild-type (WT) littermates were fed a HF diet for 3 weeks prior to whole-body metabolic assessments. Measurements were recorded every 11 min; data points shown represent the average of each 55 min interval. Data were analyzed by Student's t test. Mean RER during the dark cycle was greater in KO versus WT mice ($p < 0.01$).

muscle fatty acid oxidation play a dominant role in conferring their antidiabetic phenotype.

DISCUSSION

In this report, we show that obesity, diabetes, and HF feeding are accompanied by increased rather than decreased rates of β-oxidation in skeletal muscle and that, moreover, nutritional, pharmacologic, or genetic maneuvers that suppress mitochondrial fatty acid import protect against lipid-induced insulin resistance. The high rates of fatty acid catabolism in insulin-resistant muscles were attributed principally to "incomplete" fat oxidation, in which a large proportion of fatty acids entering the mitochondria are only partially degraded. Obesity-induced perturbations in mitochondrial fuel metabolism were further characterized by impaired switching to carbohydrate substrate and moderate depletion of several TCA cycle intermediates. Taken together, our results suggest that dietary fat is less damaging to skeletal muscle metabolic function under conditions of constrained β-oxidation.

Reciprocal regulation of fat oxidation and glucose disposal was originally described as the "glucose-fatty acid cycle" (Randle et al., 1963). Randle (1998) postulated that provision of lipid fuel promotes β-oxidation and suppresses glycolysis and pyruvate oxidation due to inhibition of hexokinase, phosphofructokinase, and pyruvate dehydrogenase. More recently, the role of this mechanism in driving insulin resistance has been discounted based on magnetic resonance spectroscopy (MRS) studies showing that concentrations of glucose and glucose-6-phosphate (the product of hexokinase) are decreased in skeletal muscle of human diabetic subjects compared to control subjects during a hyperinsulinemic-euglycemic clamp (Cline et al., 1994, 1997) and in response to prolonged lipid infusion (Dresner et al., 1999). These reports argue against the notion that reduced flux through the hexokinase reaction restricts glucose uptake in circumstances of insulin resistance and instead point toward a defect in insulin-stimulated glucose transport as the limiting factor. Indeed, numerous studies have shown that HF feeding and/or lipid exposure impair insulin signaling to GLUT4. However, lipid-mediated opposition of GLUT4 translocation could emanate from a mitochondria-derived signal, as suggested by the current study. Additionally, the foregoing MRS experiments did not assess changes in pyruvate dehydrogenase activity, which has been shown to be more potently inhibited by fatty acids than the glycolytic enzyme phosphofructokinase.

Insulin-stimulated GLUT4 translocation requires a cascade of protein phosphorylations that commence with autophosphorylation of the insulin receptor (IR) tyrosine kinase followed by tyrosine phosphorylation of its immediate substrate, insulin receptor substrate 1 (IRS-1). Both IR and IRS-1 are negatively regulated by serine phosphorylation, which opposes phosphorylation on tyrosine residues and thus impedes activation of downstream targets, including AKT and GLUT4 (Zick, 2004). Constitutive serine phosphorylation of IR and IRS has become increasingly recognized as a major molecular cause of insulin resistance (Morino et al., 2006); however, the precise biochemical events that provoke this condition remain unresolved. Strong evidence implicates a role for factors such as inflammation and endoplasmic reticulum (ER) stress (Cai et al., 2005; Ozcan et al., 2004). Additionally, much attention has focused on local

accumulation of TAG and related lipid intermediates such as DAG and LC-CoAs, which are attractive candidates because they have been shown to act as ligands for several stress-responsive serine kinases in vitro. Thus, increased levels of LC-CoAs and/or DAG might activate PKC and/or other kinases that serine phosphorylate IRS-1. In this model, diminished mitochondrial uptake and catabolism of fatty acids has been postulated as a primary metabolic insult that forces accumulation of IMTG and other lipid species (Morino et al., 2006; Zick, 2004; Yu et al., 2002).

On the other hand, our findings fit with a growing body of evidence that disassociates muscle insulin resistance from glycerolipid and/or LC-CoA content. For example, muscles from exercise-trained subjects are highly insulin sensitive despite IMTG levels that are similar or even higher than those found in association with obesity and diabetes (Goodpaster and Kelley, 2002). Furthermore, exercise intervention in type 2 diabetic patients and obese Zucker rats has been shown to improve insulin action in muscle without a corresponding decrease in LC-CoA and DAG levels (Bruce et al., 2004; Thyfault et al., 2007). Similarly, a previous study of ours found that insulin-mediated phosphorylation of AKT and GSK-3 in muscle of HF-fed rats was restored by a genetic maneuver that tended to increase IMTG and LC-CoA levels (An et al., 2004). Improved insulin signaling corresponded with a sharp decrease in muscle levels of β-OH-butyrylcarnitine, a mitochondria-derived ketone metabolite (An et al., 2004). Likewise, a 2-week exercise intervention in mice fed a chronic HF diet lowered muscle acylcarnitine levels in association with increased TCA cycle activity and complete reversal of glucose intolerance (Koves et al., 2005a). Taken together with the current report, these findings cast light on the mitochondrion as a principal target of lipid stress.

The idea that insulin resistance might stem from excessive β-oxidation agrees with numerous reports showing that lipid exposure, HF diet, and/or obesity increase expression of several β-oxidative and glucose-sparing enzymes that are targeted by the PPAR family of lipid-activated transcription factors (Gilde and Van Bilsen, 2003; Yechoor et al., 2002). Interestingly, activation of β-oxidative genes is not necessarily coordinated with increased expression of downstream metabolic pathways such as the TCA cycle and the electron transport chain. On the contrary, HF feeding and obesity result in decreased expression of PGC-1α, a transcriptional coactivator that functions as a master regulator of mitochondrial biogenesis and function (Koves et al., 2005a; Sparks et al., 2005; Mootha et al., 2003). Herein, overnutrition and/or insulin resistance lowered muscle levels of several TCA cycle intermediates, whereas ablation of *mcd* in knockout mice prevented this depletion. Thus, sustained elevations in β-oxidation and/or impaired glucose metabolism appear to reduce the TCA cycle intermediate pool. Although the functional relevance of this finding is as yet unknown, the data are congruent with previous transcriptomic analyses (Koves et al., 2005a; Sparks et al., 2005; Yechoor et al., 2002) and might reflect compromised mitochondrial status.

Consistent with our results, other genetic mouse models have likewise revealed a negative relationship between muscle β-oxidation and insulin action (Finck et al., 2005; Ibrahimi et al., 1999). For instance, muscle-specific overexpression of PPARα in transgenic mice causes both local and systemic glucose intolerance, in association with marked induction of several lipid-oxidative genes (Finck et al., 2005). The diabetic phenotype of these animals is reversed by pharmacologic inhibition of CPT1. Conversely, *PPARα* null mice have diminished β-oxidative activity and resist lipid-induced diabetes (Tordjman et al., 2001; Guerre-Millo et al., 2001). Conflicting evidence from human studies has shown both increased and decreased fat oxidation in association with obesity. Notably, however, most previous studies have been performed in the fasted state and have not assessed incomplete β-oxidation. Our studies show that unchanged rates of complete fat oxidation can be accompanied by high rates of incomplete β-oxidation. Additionally, we found that obesity-associated increases in fatty acid catabolism are most apparent in the postprandial state; this is not surprising given that normal physiological fluctuations in substrate supply dictate high rates of β-oxidation during periods of food withdrawal. In other words, the pathophysiological shift in muscle fuel selection appears to occur primarily in the fed or semi-fed state. These observations are reminiscent of previous reports showing that muscles from obese and/or diabetic subjects lose their capacity to switch between glucose and lipid substrates (Kelley et al., 1999). Our results now show that HF feeding causes a form of ''metabolic inflexibility'' that not only occurs early in the pathogenesis of disease but also is detectable in isolated mitochondria.

Importantly, the present study also provides evidence that the development and progression of insulin resistance involve a distinct set of metabolic derangements in skeletal muscle as compared to that in liver. Accordingly, the molecular mechanisms that connect lipid surplus to insulin resistance are likely to exhibit tissue specificity. In fact, the strongest evidence in favor of mechanisms involving LC-CoAs, DAG, ER stress, and/or inflammation comes from genetic models and pharmacological interventions that modulate hepatic lipid metabolism (Nagle et al., 2007; Savage et al., 2006; An et al., 2004; Dobbins et al., 2001; Cai et al., 2005; Ozcan et al., 2004). Relevant to the present study, knockout mice lacking acetyl-CoA carboxylase 2 have decreased tissue levels of malonyl-CoA and resist diet-induced obesity and diabetes (Abu-Elheiga et al., 2003), seemingly in conflict with our results. However, these mice exhibit only minor adjustments in muscle lipid metabolism but profound changes in liver lipid metabolism, as evidenced by marked increases in hepatic β-oxidation and ketogenesis and protection against hepatic steatosis. Thus, in this as in other similar studies (An et al., 2004; Nagle et al., 2007), the liver appears to serve as a catabolic sink that protects against systemic hyperlipidemia.

In contrast to skeletal muscle, the liver harbors robust capacity to repackage and export fatty acids, not only in the form of very low-density lipoprotein (VLDL)-TAG but also as ketones, which are generated by liver mitochondria when reducing potential is high. Conversely, anabolic pathways such as lipogenesis, gluconeogenesis, glycerolipid synthesis, and ketogenesis are relatively inactive in muscle. We therefore suggest that muscle mitochondria are particularly vulnerable to energy overload and, as such, serve as the principal lipid sensors of this tissue. This paradigm fits with emerging data linking diabetes to muscle mitochondrial dysfunction (Morino et al., 2006) and evidence that exercise-induced reversal of insulin resistance correlates with improved mitochondrial performance (Koves et al., 2005a; Menshikova et al., 2005).

Lastly, our results prompt speculation of a mitochondria-derived signal that couples incomplete β-oxidation to insulin resistance. Perhaps specific acylcarnitine esters function as signaling molecules and/or participate in processes related to protein acetylation/acylation. In support of this possibility, a recent proteomics report identified several mitochondrial proteins that appear to be regulated by nutrient-induced changes in acetylation state (Kim et al., 2006). We emphasize, however, that the acylcarnitines per se may not play a direct role in mediating insulin resistance. In the context of inborn mitochondrial diseases, acylcarnitine production has been viewed as a detoxifying system that permits mitochondrial efflux of excess acyl groups (Ramsay, 2000). Thus, muscle accumulation of these intermediates could reflect a failed attempt to alleviate reductive and/or oxidative stress caused by mitochondrial overload (Andreyev et al., 2005). Notably, reactive oxygen species are known to activate several of the serine kinases that target IRS-1 (Bloch-Damti and Bashan, 2005), and recent reports have implicated both oxidative and reductive stress as potential diabetogenic culprits (Houstis et al., 2006; Parikh et al., 2007). These are attractive scenarios that could explain insulin resistance provoked by oversupply of any metabolic substrate.

In summary, our report links skeletal muscle insulin resistance to lipid-induced mitochondrial stress. We propose that HF feeding results in excessive β-oxidation, due to both PPAR-mediated transcriptional remodeling and increased supply of lipid substrate (Figure S7). In the absence of work (i.e., physical activity), the TCA cycle not only remains inactivated at a transcriptional level but is constrained by redox pressure and depletion of supporting intermediates. This imbalanced environment appears to exacerbate incomplete β-oxidation and encourage intramitochondrial accumulation of acyl-CoAs, their respective acylcarnitines, and perhaps other as yet unidentified metabolites that could contribute to mitochondrial failure. These findings suggest that drugs designed to enhance CPT1 activity and/or fat oxidation might alleviate metabolic derangements in liver but exacerbate those in muscle.

EXPERIMENTAL PROCEDURES

Animal Studies

All animal studies were approved by the Duke University Institutional Animal Care and Use Committee or the University of Alberta Animal Policy and Welfare Committee. Male Wistar rats (300 g; Harlan) were housed in a temperature-controlled environment with a 12:12 hr light/dark cycle and provided ad libitum access to standard chow (SC) (7001; Harlan Teklad) or a 45% high-fat (HF) diet (D12451; Research Diets) and water. Male ZDF and lean littermate rats were purchased from Charles River Laboratories. Tissues were harvested at 12 weeks of age, after the onset of frank diabetes and hyperlipidemia as assessed by fasting blood levels of glucose, insulin, triglycerides, and NEFA. On the day of experiments, food was removed either 4 hr (fed) or 24 hr (fasted) before anesthesia was administered. *mcd*$^{-/-}$ mice (Dyck et al., 2006) and wild-type littermates were fed either a low-fat (10%) or high-fat (60%) diet (D12492; Research Diets) for 12 weeks. Glucose and insulin tolerance tests were performed 6 hr after food withdrawal using glucose and insulin doses of 2 g/kg and 0.3 U/kg, respectively.

Plasma Measures

EDTA plasma was collected after feeding, after overnight fast, and at the time of sacrifice and was analyzed for triacylglycerides (#337-B; Sigma), NEFA (NEFA C kit; Wako Chemicals), insulin (EZRMI-13K; Millipore), leptin (XL85-K; Millipore), and corticosteroids (80100; Diagnostic Systems Laboratories, Inc.).

Metabolite Profiling

Mass spectrometry-based metabolic profiling was performed as described previously (An et al., 2004; Haqq et al., 2005). Further details are provided in Supplemental Experimental Procedures.

Muscle Homogenate and Mitochondrial Oxidation

Deep (red) quadriceps, superficial (white) quadriceps, and gastrocnemius muscles were excised from anesthetized rats and placed in ice-cold modified Chappell-Perry buffer. Muscle homogenates were prepared from ~100 mg quadriceps samples as described previously (Kim et al., 2002). One gastrocnemius muscle was immediately flash frozen for metabolic profiling, and the contralateral muscle was used for mitochondrial isolations as described previously (Koves et al., 2005b); subsarcolemmal and intermyofibrillar pellets were combined. Oxidation studies were performed using 0.2 mM [1-^{14}C]oleate in the absence or presence of 2 mM sodium pyruvate using methods described in Kim et al. (2002). Reactions were terminated by adding 100 μl 70% perchloric acid, and $^{14}CO_2$ was trapped in 200 μl of 1 N NaOH. $^{14}CO_2$ and ^{14}C-labeled acid-soluble metabolites were assessed by liquid scintillation counting in Uniscint BD (National Diagnostics).

Cultured Myocytes

L6 myoblasts (ATCC) were grown in DMEM with 10% FBS and induced to differentiate by switching to DMEM containing 2% horse serum as described previously (Muoio et al., 2002). Mature myotubes were treated for 24 hr with vehicle (0.5% BSA) and/or fatty acids and 0–2.0 mM L-carnitine and then harvested for assessment of triacylglycerides (GPO-Trinder kit; Sigma) and protein (BCA assay kit; Pierce) and metabolic profiling. For signaling studies, L6 cells were harvested 10 min after addition of 100 nM insulin. Lysates were immediately homogenized in loading buffer consisting of 20 mM Tris-HCl (ph 7.5), 20% glycerol, 0.02% bromophenol blue, 5% β-mercaptoethanol, and 4% SDS supplemented with phosphatase and protease inhibitor cocktails (Sigma-Aldrich). Thirty micrograms of total cell protein was separated on 10% Criterion gel (Bio-Rad) and transferred to nitrocellulose before blocking and probing using antibodies against phospho-Akt (Ser473) (1:1,000; Cell Signaling Technology), total Akt (1:1,000; Cell Signaling Technology), or β-tubulin (1:20,000; Sigma). MemCode stain (Pierce) was used to normalize protein transfer. Proteins were visualized using horseradish peroxidase-conjugated immunoglobulin G antibodies and an ECL Plus chemiluminescence detection kit and quantified using ImageQuant Software (Amersham Biosciences).

Statistics

Data were analyzed by two-tailed Student's t test or two-way ANOVA when appropriate using JMP software version 6 (SAS Institute Inc.). ANOVA was performed on data at a minimum $p < 0.05$ threshold, and Tukey's HSD post hoc test was performed to evaluate differences between treatment groups. Multivariate fitting to examine the effect of diet or genotype on organic acids and acylcarnitines was performed by MANOVA using identity as the response design.

Supplemental Data

Supplemental Data include Supplemental Experimental Procedures, Supplemental References, one table, and seven figures and can be found with this article online at http://www.cellmetabolism.org/cgi/content/full/7/1/45/DC1/.

ACKNOWLEDGMENTS

We thank the dedicated staff of the Metabolomics and Biomarker Core of the Sarah W. Stedman Nutrition and Metabolism Center. These studies were supported by NIH grants K01-DK56112 (D.M.M.) and P01-DK58398 (C.B.N.), the American Diabetes Association (D.M.M.), and a Duke University John A. Hartford Center for Excellence junior faculty award (T.R.K.). G.D.L. is funded by grant support from the Canadian Institutes of Health Research (CIHR), and J.R.B.D. is funded by grants from the Canadian Diabetes Association and the CIHR. G.D.L. and J.R.B.D. are shareholders and officers of Metabolic Modulators Research Ltd., a company with commercial interests in the development of MCD inhibitors.

Received: May 9, 2007
Revised: July 27, 2007
Accepted: October 23, 2007
Published: January 8, 2008

REFERENCES

Abu-Elheiga, L., Oh, W., Kordari, P., and Wakil, S.J. (2003). Acetyl-CoA carboxylase 2 mutant mice are protected against obesity and diabetes induced by high-fat/high-carbohydrate diets. Proc. Natl. Acad. Sci. USA *100*, 10207–10212.

An, J., Muoio, D.M., Shiota, M., Fujimoto, Y., Cline, G.W., Shulman, G.I., Koves, T.R., Stevens, R., Millington, D., and Newgard, C.B. (2004). Hepatic expression of malonyl-CoA decarboxylase reverses muscle, liver and whole-animal insulin resistance. Nat. Med. *10*, 268–274.

Andreyev, A.Y., Kushnareva, Y.E., and Starkov, A.A. (2005). Mitochondrial metabolism of reactive oxygen species. Biochemistry (Mosc.) *70*, 200–214.

Bloch-Damti, A., and Bashan, N. (2005). Proposed mechanisms for the induction of insulin resistance by oxidative stress. Antioxid. Redox Signal. *7*, 1553–1567.

Bruce, C.R., Kriketos, A.D., Cooney, G.J., and Hawley, J.A. (2004). Disassociation of muscle triglyceride content and insulin sensitivity after exercise training in patients with Type 2 diabetes. Diabetologia *47*, 23–30.

Cai, D., Yuan, M., Frantz, D.F., Melendez, P.A., Hansen, L., Lee, J., and Shoelson, S.E. (2005). Local and systemic insulin resistance resulting from hepatic activation of IKK-beta and NF-kappaB. Nat. Med. *11*, 183–190.

Chavez, J.A., Knotts, T.A., Wang, L.P., Li, G., Dobrowsky, R.T., Florant, G.L., and Summers, S.A. (2003). A role for ceramide, but not diacylglycerol, in the antagonism of insulin signal transduction by saturated fatty acids. J. Biol. Chem. *278*, 10297–10303.

Cline, G.W., Rothman, D.L., Magnusson, I., Katz, L.D., and Shulman, G.I. (1994). 13C-nuclear magnetic resonance spectroscopy studies of hepatic glucose metabolism in normal subjects and subjects with insulin-dependent diabetes mellitus. J. Clin. Invest. *94*, 2369–2376.

Cline, G.W., Magnusson, I., Rothman, D.L., Petersen, K.F., Laurent, D., and Shulman, G.I. (1997). Mechanism of impaired insulin-stimulated muscle glucose metabolism in subjects with insulin-dependent diabetes mellitus. J. Clin. Invest. *99*, 2219–2224.

Dobbins, R.L., Szczepaniak, L.S., Bentley, B., Esser, V., Myhill, J., and McGarry, J.D. (2001). Prolonged inhibition of muscle carnitine palmitoyltransferase-1 promotes intramyocellular lipid accumulation and insulin resistance in rats. Diabetes *50*, 123–130.

Dresner, A., Laurent, D., Marcucci, M., Griffin, M.E., Dufour, S., Cline, G.W., Slezak, L.A., Andersen, D.K., Hundal, R.S., Rothman, D.L., et al. (1999). Effects of free fatty acids on glucose transport and IRS-1-associated phosphatidylinositol 3-kinase activity. J. Clin. Invest. *103*, 253–259.

Dyck, J.R., Hopkins, T.A., Bonnet, S., Michelakis, E.D., Young, M.E., Watanabe, M., Kawase, Y., Jishage, K., and Lopaschuk, G.D. (2006). Absence of malonyl coenzyme A decarboxylase in mice increases cardiac glucose oxidation and protects the heart from ischemic injury. Circulation *114*, 1721–1728.

Finck, B.N., Bernal-Mizrachi, C., Han, D.H., Coleman, T., Sambandam, N., LaRiviere, L., Holloszy, J.O., Semenkovich, C.F., and Kelly, D.P. (2005). A potential link between muscle peroxisome proliferator-activated receptor-alpha signaling and obesity-related diabetes. Cell Metab. *1*, 133–144.

Gilde, A.J., and Van Bilsen, M. (2003). Peroxisome proliferator-activated receptors (PPARS): regulators of gene expression in heart and skeletal muscle. Acta Physiol. Scand. *178*, 425–434.

Goodpaster, B.H., and Kelley, D.E. (2002). Skeletal muscle triglyceride: marker or mediator of obesity-induced insulin resistance in type 2 diabetes mellitus? Curr. Diab. Rep. *2*, 216–222.

Guerre-Millo, M., Rouault, C., Poulain, P., Andre, J., Poitout, V., Peters, J.M., Gonzalez, F.J., Fruchart, J.C., Reach, G., and Staels, B. (2001). PPAR-alpha-null mice are protected from high-fat diet-induced insulin resistance. Diabetes *50*, 2809–2814.

Haqq, A.M., Lien, L.F., Boan, J., Arlotto, M., Slentz, C.A., Muehlbauer, M.J., Rochon, J., Gallup, D., McMahon, R.L., Bain, J.R., et al. (2005). The Study of the Effects of Diet on Metabolism and Nutrition (STEDMAN) weight loss project: Rationale and design. Contemp. Clin. Trials *26*, 616–625.

Holland, W.L., Brozinick, J.T., Wang, L.P., Hawkins, E.D., Sargent, K.M., Liu, Y., Narra, K., Hoehn, K.L., Knotts, T.A., Siesky, A., et al. (2007). Inhibition of ceramide synthesis ameliorates glucocorticoid-, saturated-fat-, and obesity-induced insulin resistance. Cell Metab. *5*, 167–179.

Houstis, N., Rosen, E.D., and Lander, E.S. (2006). Reactive oxygen species have a causal role in multiple forms of insulin resistance. Nature *440*, 944–948.

Hulver, M.W., Berggren, J.R., Cortright, R.N., Dudek, R.W., Thompson, R.P., Pories, W.J., MacDonald, K.G., Cline, G.W., Shulman, G.I., Dohm, G.L., and Houmard, J.A. (2003). Skeletal muscle lipid metabolism with obesity. Am. J. Physiol. Endocrinol. Metab. *284*, E741–E747.

Ibrahimi, A., Bonen, A., Blinn, W.D., Hajri, T., Li, X., Zhong, K., Cameron, R., and Abumrad, N.A. (1999). Muscle-specific overexpression of FAT/CD36 enhances fatty acid oxidation by contracting muscle, reduces plasma triglycerides and fatty acids, and increases plasma glucose and insulin. J. Biol. Chem. *274*, 26761–26766.

Kelley, D.E., Goodpaster, B., Wing, R.R., and Simoneau, J.A. (1999). Skeletal muscle fatty acid metabolism in association with insulin resistance, obesity, and weight loss. Am. J. Physiol. *277*, E1130–E1141.

Kim, J.Y., Koves, T.R., Yu, G.S., Gulick, T., Cortright, R.N., Dohm, G.L., and Muoio, D.M. (2002). Evidence of a malonyl-CoA-insensitive carnitine palmitoyltransferase I activity in red skeletal muscle. Am. J. Physiol. Endocrinol. Metab. *282*, E1014–E1022.

Kim, S.C., Sprung, R., Chen, Y., Xu, Y., Ball, H., Pei, J., Cheng, T., Kho, Y., Xiao, H., Xiao, L., et al. (2006). Substrate and functional diversity of lysine acetylation revealed by a proteomics survey. Mol. Cell *23*, 607–618.

Koves, T.R., Li, P., An, J., Akimoto, T., Slentz, D., Ilkayeva, O., Dohm, G.L., Yan, Z., Newgard, C.B., and Muoio, D.M. (2005a). Peroxisome proliferator-activated receptor-gamma co-activator 1alpha-mediated metabolic remodeling of skeletal myocytes mimics exercise training and reverses lipid-induced mitochondrial inefficiency. J. Biol. Chem. *280*, 33588–33598.

Koves, T.R., Noland, R.C., Bates, A.L., Henes, S.T., Muoio, D.M., and Cortright, R.N. (2005b). Subsarcolemmal and intermyofibrillar mitochondria play distinct roles in regulating skeletal muscle fatty acid metabolism. Am. J. Physiol. Cell Physiol. *288*, C1074–C1082.

Lee, J.S., Pinnamaneni, S.K., Eo, S.J., Cho, I.H., Pyo, J.H., Kim, C.K., Sinclair, A.J., Febbraio, M.A., and Watt, M.J. (2006). Saturated, but not n-6 polyunsaturated, fatty acids induce insulin resistance: role of intramuscular accumulation of lipid metabolites. J. Appl. Physiol. *100*, 1467–1474.

Menshikova, E.V., Ritov, V.B., Toledo, F.G., Ferrell, R.E., Goodpaster, B.H., and Kelley, D.E. (2005). Effects of weight loss and physical activity on skeletal muscle mitochondrial function in obesity. Am. J. Physiol. Endocrinol. Metab. *288*, E818–E825.

Monetti, M., Levin, M.C., Watt, M.J., Sajan, M.P., Marmor, S., Hubbard, B.K., Stevens, R.D., Bain, J.R., Newgard, C.B., Farese, R.V., Sr., et al. (2007). Dissociation of hepatic steatosis and insulin resistance in mice overexpressing DGAT in the liver. Cell Metab. *6*, 69–78.

Mootha, V.K., Lindgren, C.M., Eriksson, K.F., Subramanian, A., Sihag, S., Lehar, J., Puigserver, P., Carlsson, E., Ridderstrale, M., Laurila, E., et al. (2003). PGC-1alpha-responsive genes involved in oxidative phosphorylation are coordinately downregulated in human diabetes. Nat. Genet. *34*, 267–273.

Morino, K., Petersen, K.F., and Shulman, G.I. (2006). Molecular mechanisms of insulin resistance in humans and their potential links with mitochondrial dysfunction. Diabetes *55* (*Suppl 2*), S9–S15.

Muoio, D.M., and Newgard, C.B. (2006). Obesity-related derangements in metabolic regulation. Annu. Rev. Biochem. *75*, 367–401.

Muoio, D.M., MacLean, P.S., Lang, D.B., Li, S., Houmard, J.A., Way, J.M., Winegar, D.A., Corton, J.C., Dohm, G.L., and Kraus, W.E. (2002). Fatty acid homeostasis and induction of lipid regulatory genes in skeletal muscles of peroxisome proliferator-activated receptor (PPAR) alpha knock-out mice. Evidence for compensatory regulation by PPAR delta. J. Biol. Chem. *277*, 26089–26097.

Nagle, C.A., An, J., Shiota, M., Torres, T.P., Cline, G.W., Liu, Z.X., Wang, S., Catlin, R.L., Shulman, G.I., Newgard, C.B., and Coleman, R.A. (2007). Hepatic overexpression of glycerol-sn-3-phosphate acyltransferase 1 in rats causes insulin resistance. J. Biol. Chem. *282*, 14807–14815.

Ozcan, U., Cao, Q., Yilmaz, E., Lee, A.H., Iwakoshi, N.N., Ozdelen, E., Tuncman, G., Gorgun, C., Glimcher, L.H., and Hotamisligil, G.S. (2004). Endoplasmic reticulum stress links obesity, insulin action, and type 2 diabetes. Science *306*, 457–461.

Parikh, H., Carlsson, E., Chutkow, W.A., Johansson, L.E., Storgaard, H., Poulsen, P., Saxena, R., Ladd, C., Schulze, P.C., Mazzini, M.J., et al. (2007). TXNIP regulates peripheral glucose metabolism in humans. PLoS Med. *4*, e158.

Rachek, L.I., Musiyenko, S.I., LeDoux, S.P., and Wilson, G.L. (2007). Palmitate induced mitochondrial deoxyribonucleic acid damage and apoptosis in l6 rat skeletal muscle cells. Endocrinology *148*, 293–299.

Ramsay, R.R. (2000). The carnitine acyltransferases: modulators of acyl-CoA-dependent reactions. Biochem. Soc. Trans. *28*, 182–186.

Randle, P.J. (1998). Regulatory interactions between lipids and carbohydrates: the glucose fatty acid cycle after 35 years. Diabetes Metab. Rev. *14*, 263–283.

Randle, P.J., Garland, P.B., Hales, C.N., and Newsholme, E.A. (1963). The glucose fatty-acid cycle. Its role in insulin sensitivity and the metabolic disturbances of diabetes mellitus. Lancet *1*, 785–789.

Ruderman, N.B., Saha, A.K., Vavvas, D., and Witters, L.A. (1999). Malonyl-CoA, fuel sensing, and insulin resistance. Am. J. Physiol. *276*, E1–E18.

Savage, D.B., Choi, C.S., Samuel, V.T., Liu, Z.X., Zhang, D., Wang, A., Zhang, X.M., Cline, G.W., Yu, X.X., Geisler, J.G., et al. (2006). Reversal of diet-induced hepatic steatosis and hepatic insulin resistance by antisense oligonucleotide inhibitors of acetyl-CoA carboxylases 1 and 2. J. Clin. Invest. *116*, 817–824.

Sparks, L.M., Xie, H., Koza, R.A., Mynatt, R., Hulver, M.W., Bray, G.A., and Smith, S.R. (2005). A high-fat diet coordinately downregulates genes required for mitochondrial oxidative phosphorylation in skeletal muscle. Diabetes *54*, 1926–1933.

Thyfault, J.P., Cree, M.G., Zheng, D., Zwetsloot, J.J., Tapscott, E.B., Koves, T.R., Ilkayeva, O., Wolfe, R.R., Muoio, D.M., and Dohm, G.L. (2007). Contraction of insulin-resistant muscle normalizes insulin action in association with increased mitochondrial activity and fatty acid catabolism. Am. J. Physiol. Cell Physiol. *292*, C729–C739. Published online October 18, 2006. 10.1152/ajpcell.00311.2006.

Tordjman, K., Bernal-Mizrachi, C., Zemany, L., Weng, S., Feng, C., Zhang, F., Leone, T.C., Coleman, T., Kelly, D.P., and Semenkovich, C.F. (2001). PPARalpha deficiency reduces insulin resistance and atherosclerosis in apoE-null mice. J. Clin. Invest. *107*, 1025–1034.

Van Hove, J.L., Zhang, W., Kahler, S.G., Roe, C.R., Chen, Y.T., Terada, N., Chace, D.H., Iafolla, A.K., Ding, J.H., and Millington, D.S. (1993). Medium-chain acyl-CoA dehydrogenase (MCAD) deficiency: diagnosis by acylcarnitine analysis in blood. Am. J. Hum. Genet. *52*, 958–966.

Yechoor, V.K., Patti, M.E., Saccone, R., and Kahn, C.R. (2002). Coordinated patterns of gene expression for substrate and energy metabolism in skeletal muscle of diabetic mice. Proc. Natl. Acad. Sci. USA *99*, 10587–10592.

Yu, C., Chen, Y., Cline, G.W., Zhang, D., Zong, H., Wang, Y., Bergeron, R., Kim, J.K., Cushman, S.W., Cooney, G.J., et al. (2002). Mechanism by which fatty acids inhibit insulin activation of insulin receptor substrate-1 (IRS-1)-associated phosphatidylinositol 3-kinase activity in muscle. J. Biol. Chem. *277*, 50230–50236.

Zick, Y. (2004). Uncoupling insulin signalling by serine/threonine phosphorylation: a molecular basis for insulin resistance. Biochem. Soc. Trans. *32*, 812–816.